INFECTION AND IMMUNITY, June 2004, p. 3609–3621 Vol. 72, No. 6
0019-9567/04/$08.00+0 DOI: 10.1128/IAI.72.6.3609–3621.2004

The Serine Protease Motif of EspC from Enteropathogenic *Escherichia coli* Produces Epithelial Damage by a Mechanism Different from That of Pet Toxin from Enteroaggregative *E. coli*

Fernando Navarro-García,[1]* Adrián Canizalez-Roman,[1] Bao Quan Sui,[2] James P. Nataro,[2] and Yenia Azamar[1]

Department of Cell Biology, CINVESTAV-IPN, 07000 México DF, Mexico,[1] and Center for Vaccine Development, University of Maryland School of Medicine, Baltimore, Maryland 21201[2]

Received 15 December 2003/Returned for modification 9 February 2004/Accepted 21 February 2004

EspC (*Escherichia coli* secreted protein C) of enteropathogenic *E. coli* (EPEC) shows the three classical domains of the autotransporter proteins and has a conserved serine protease motif belonging to the SPATE (serine protease autotransporters of *Enterobacteriaceae*) subfamily. EspC and its homolog Pet in enteroaggregative *E. coli* (EAEC) bear the same sequence within the serine protease motif, and both proteins produce enterotoxic effects, suggesting that like Pet, EspC could be internalized to reach and cleave the calmodulin-binding domain of fodrin, causing actin cytoskeleton disruption. Even though both proteins cause cytoskeleton damage by virtue of their serine protease motifs, the following evidence supports the hypothesis that the mechanisms are different. (i) To obtain similar cytotoxic and cytoskeletal effects, a threefold-higher EspC concentration and a twofold-higher exposure time are needed. (ii) EspC internalization into epithelial cells takes more time (6 h) than Pet internalization (30 min), and the distributions of the two proteins inside the cells are also different. (iii) Both proteins have affinity for fodrin and cleave it, but the cleavage sites are different; EspC produces two cleavages, while Pet produces just one. (iv) EspC does not cause fodrin redistribution within epithelial cells. (v) An EspC serine protease motif mutant, but not a Pet serine protease mutant, competes with EspC by blocking cytoskeletal damage. All these data suggest that the protein conformational structure is very important for the activity of the catalytic site, influencing its interaction with the target protein and its internalization. The differences between these proteins may explain the reduced ability of EspC to cause cytopathic effects. However, these differences may confer a specialized role on EspC in the pathogenesis of EPEC, which is different from that of Pet in EAEC pathogenesis.

Enteropathogenic *Escherichia coli* (EPEC), a leading cause of infantile diarrhea in developing countries, secretes effector molecules which allow bacteria to interact with their hosts and cause disease (7, 11). EPEC secretes at least six proteins (Esp [*E. coli* secreted proteins]), four of which, EspA (11), EspD (14), EspB (26), and EspF (16), are secreted by a type III secretion system. Esp molecules as well as the secretion apparatus are encoded within a 35.6-kb pathogenicity island termed the locus of enterocyte effacement (LEE) (4, 15). EspA, EspD, and EspB proteins form a translocon for delivering effector molecules into the host cytosol (12, 22). Tir (translocated intimin receptor) is translocated through this apparatus (10) and serves as a receptor for the EPEC adhesin intimin (9). Intimin is required for intimate bacterial attachment to host cells (8) and to focus the polymerization of cytoskeletal rearrangements leading to the disruption of intestinal microvilli, a phenotype known as the attaching and effacing (A/E) lesion (18).

In addition to the secretion of the proteins via the type III secretion system mentioned above, EPEC also secretes a protein via the type V secretion system, the autotransporter pathway (25). This protein, EspC, shows the three classical domains (signal peptide, passenger domain, and β-domain) of the autotransporter proteins, which were first described for the immunoglobulin A (IgA) protease of *Neisseria gonorrhoeae* (23, 25). EspC also has a conserved serine protease motif similar to the IgA protease but does not cleave IgA, as do several other members of the autotransporter family of proteins. In fact, EspC belongs to the subfamily of serine protease autotransporters of *Enterobacteriaceae* (SPATE) including Tsh, SepA, Pic, EspP, Sat, and Pet; none of these cleave IgA. Moreover, the catalytic serine endopeptidase, which has autoproteolytic activity to cleave off the mature IgA protease, is not necessary for release of EspC into the extracellular space, as with other SPATE members, including Pet. The presence of sequences homologous to *espC* in the pathogenic strains of RDEC-1, *Citrobacter freundii*, and *Hafnia alvei* but not in nonpathogenic strains implies that EspC may have a role in the virulence of A/E-inducing pathogens (25). However, an *espC* deletion mutant constructed by allelic exchange is indistinguishable from its isogenic parent in adherence, invasion, actin rearrangement, and Tir phosphorylation, events which are crucial for A/E lesion formation (25). Recently, we have determined that *espC* is located within a second EPEC pathogenicity island at 60 min on the chromosome of *E. coli*. Moreover, we found that EspC has enterotoxic activity on intestinal segments mounted in Ussing chambers and that this activity is abolished by preincubation with an antiserum against the homologous Pet enterotoxin of enteroaggregative *E. coli* (EAEC) (17), which displays 55% identity (70% similarity).

* Corresponding author. Mailing address: Department of Cell Biology, CINVESTAV-IPN, Ap. Postal 14-740, 07000 México, DF, Mexico. Phone: (52-55) 5061-3990. Fax: (52-55) 5747-7081. E-mail: fnavarro@cell.cinvestav.mx.

Pet toxin has enterotoxic (20) and cytotoxic activities on epithelial cells, activities related to its serine protease motif, since a mutant with a site-directed mutation in this motif prevents both activities, and a serine protease inhibitor (phenylmethylsulfonyl fluoride [PMSF]) also inhibits the cytotoxic activity (21). Both the serine protease inhibitor and the serine protease mutant abolish degradation of the target protein, epithelial fodrin (1). Recently, it has also been found that Pet internalization is required to produce the cytoskeletal damage which leads to the cytotoxic effect (19) as a consequence of fodrin disruption (1). Thus, three critical steps are needed for the cytotoxic effects caused by Pet: (i) the active serine protease motif, (ii) uptake of Pet by the epithelial cells, and (iii) fodrin disruption. The fact that EspC and Pet bear exactly the same sequence within the serine protease motif (GDSGSG), in contrast with other members of the SPATE subfamily, and that both produce enterotoxic effects suggested that EspC of EPEC could cause epithelial cell damage by the same mechanism as Pet of EAEC. In this work we show the effects of EspC on epithelial cells, with emphasis on those produced by its homologous Pet toxin.

MATERIALS AND METHODS

Strains and plasmids. The minimal *espC* clone pJLM174, previously described, was constructed by cloning the *espC* gene of EPEC strain E2348/69 into the EcoRI/HindIII site of pBAD30 and was expressed in *E. coli* HB101 (17). HB101(pJLM174), grown in Luria broth supplemented with 0.2% glycerol and 0.2% arabinose, was used to obtain EspC protein, and supernatant proteins from HB101(pJML174) grown in Luria broth supplemented with 0.2% glucose (no EspC expression) were used as controls. The minimal *pet* clone pCEFN1, previously described, was constructed by cloning the *pet* gene of EAEC strain 042 into the BamHI/KpnI site of pSPORT1 and was expressed in *E. coli* HB101 (5); supernatant proteins from HB101(pSPORT1) were used as controls. Clone 18531, representing bp 2531 to 4689 of human αII spectrin, was kindly provided by Paul A. Stabatch and Jon S. Morrow (24); it was cloned into pBluescript by using EcoRI adapters and subcloned into the EcoRI site of the inducible bacterial expression vector pGEX-3X (Pharmacia). The strains were maintained on L agar or in L broth containing 100 μg of ampicillin/ml.

Site-directed mutagenesis. Site-directed mutagenesis was performed using the QuikChange site-directed mutagenesis kit from Stratagene (La Jolla, Calif.). A set of synthetic oligonucleotides (accession no. AF297061) was used to produce EspC S256I, as had been done previously to produce Pet S260I (21). Briefly, the set of oligonucleotides encoded an isoleucine to replace the serine at residue 256 of the serine protease motif of the EspC passenger domain. Directed mutagenesis was performed on the minimal clone pJLM174 according to the manufacturer's instructions by using *PfuTurbo* DNA polymerase.

Preparation of recombinant proteins. Broth cultures of the *espC*, *pet*, EspC S256I, or Pet S260I minimal clones in HB101 were incubated overnight at 37°C and then centrifuged at 7,000 × *g* for 15 min. The culture supernatants were filtered through 0.22-μm-pore-size cellulose acetate membrane filters (Corning, Cambridge, Mass.), concentrated 100-fold in an ultrafree centrifugal filter device with a 100-kDa cutoff (Millipore, Bedford, Mass.), filter sterilized again, and stored at −20°C for as long as 3 months.

Glutathione *S*-transferase (GST)-fodrin was prepared as described previously (24). Briefly, overnight bacterial cultures from clone 18531 expressed in BL21 were diluted 1:10 in fresh medium, grown for 1 h, and then induced for 1 to 3 h with isopropyl-β-D-thiogalactopyranoside (IPTG) before being harvested by centrifugation. Lysis was achieved by gently agitating the bacterial pellet for 30 min at 4°C in 100 μl of a solution containing 40 mM Tris-HCl (pH 7.5), 100 mM NaCl, 1 mM dithiothreitol (DTT), 1 mg of lysozyme/ml, and a protease inhibitor cocktail (Complete; Boehringer, Mannheim, Germany), after which the samples were frozen at −70°C and rapidly thawed at 30°C. Triton X-100 was added to a final concentration of 1% (vol/vol), and the sample was incubated at 4°C for an additional 30 min and then sonicated three times for 10 s each time. The 15,000 ×*g* supernatant of the lysate was affinity absorbed on 20 μl of glutathione-Sepharose 4B beads (Pharmacia) at 4°C and washed five times with 2 ml of phosphate-buffered saline solution (PBS) with 1 mM DTT. The bound peptide was eluted in 40 μl of the same buffer containing 10 mM glutathione.

Preparation of polyclonal antibodies. Antibodies against either EspC or GST were elicited by using purified proteins as described above and injecting the proteins into rabbits or mice, respectively. Antibody responses and specificities were determined by immunoblotting, and the gamma fractions from the antisera were diluted according to their sensitivity.

Cell culture. HEp-2 cells were propagated in a humidified atmosphere of 5% CO_2–95% air at 37°C in Dulbecco's modified Eagle's medium (DMEM) supplemented with 5% fetal bovine serum (HyClone, Logan, Utah), 1% nonessential amino acids, 5 mM L-glutamine, penicillin (100 U/ml), and streptomycin (100 μg/ml). Subcultures were serially propagated after being harvested with 10 mM EDTA and 0.25% trypsin (GIBCO BRL, Grand Island, N.Y.) in PBS (pH 7.4). For experimental use, subconfluent HEp-2 cells were resuspended with EDTA-trypsin, plated into eight-well LabTek slides (VWR, Bridgeport, N.J.), and allowed to grow to ca. 60% confluence (about 2 days).

Tissue culture assay. For all experiments, concentrated filtrates containing mutant or native EspC or Pet were directly diluted into tissue culture medium overlaid on the cells (without antibiotics or serum) at a final volume of 250 μl per well (for eight-well LabTek slides). For competition experiments, cells were treated with either Pet S260I (70 μg/ml) or EspC S256I (220 μg/ml) for 30 min and then with either Pet (37 μg/ml) for 3 h or EspC (120 μg/ml) for 9 h. Following the specified incubation times in a humidified atmosphere of 10% CO_2–90% air at 37°C, the medium was aspirated, and cells were washed twice with PBS and processed by the methods described below.

(i) Giemsa staining. Cells were fixed with 70% methanol and stained with a 10% Giemsa stain (Sigma). Slides were analyzed at a magnification of ×100 with standard bright-field light microscopy. Toxic activity (defined as altered HEp-2 cell morphology) was scored by using a modified scale from previous work (21).

(ii) FAS assay. A fluorescence actin-staining (FAS) assay was performed as described by Knutton et al. (13). Cells were fixed with 2% formalin–PBS, washed, permeabilized by addition of 0.1% Triton X-100–PBS, and stained with 0.05 μg of tetramethyl rhodamine isothiocyanate (TRITC)-phalloidin/ml. Slides were mounted on Gelvatol, covered with glass coverslips, and examined under confocal microscopy.

(iii) Immunostaining. Cells were fixed with 2% formalin–PBS, washed, permeabilized by addition of 0.1% Triton X-100–PBS, stained with 0.05 μg of TRITC-phalloidin/ml, and incubated with the appropriate antibody (anti-EspC, anti-Pet, or anti-spectrin α II [C-20]; Santa Cruz Biotech, Santa Cruz, Calif.). The antigen-antibody reaction was developed by using the appropriate secondary antibody (fluorescein-labeled goat anti-rabbit IgG or donkey anti-goat IgG). Slides were mounted on Gelvatol, covered with glass coverslips, and examined under a Leica TCS SP2 confocal microscope.

PCR for pcDNA3.1/CT-GFP-*espC* plasmid construction. For pcDNA3.1/CT-GFP-*espC* construction, primers were designed to generate the functional domain part of EspC in frame with the cycle 3 GFP stop codon TAA; the sense primer was 5′-GCGGCCGC**ATG**GCTCAACTAAATATTGATAATGTATG-3′, and the antisense primer was 5′-GATTGACCTCTGTCAGGAAGGATTTAT-3′. The sense primer contained a NotI cleavage site (underlined) and an ATG start codon (boldfaced). Amplifications were performed by using 0.2 mM deoxynucleoside triphosphates, 0.2 μM each primer, 500 ng of the purified plasmid pJLM174 (17) as a template, 2.5 mM $MgCl_2$, 1× buffer, and 1 U of *Pfu* Turbo DNA polymerase (Stratagene, Inc.). The reaction mixture was subjected to initial denaturation for 2 min at 94°C, followed by 35 amplification cycles of 94°C for 30 s, 60°C for 30 s, and 72°C for 1 min, 30 s; the final step was carried out at 72°C for 5 min. PCR products were purified, and a 3′ adenine was added to each fragment by one-step incubation at 72°C for 20 min using 0.2 mM deoxynucleoside triphosphates, 2.5 mM $MgCl_2$, 1× buffer, and 0.2 U of *Taq* DNA polymerase (Promega). This product was purified and inserted into pcDNA3.1/CT-GFP-TOPO. The construct was verified by NotI digestion and DNA sequence analysis in the Biopolymer Laboratory, Department of Microbiology and Immunology, University of Maryland School of Medicine.

Transfection. Transfection was carried out according to the manufacturer's instructions (Invitrogen). Briefly, 0.25 μg of plasmid and 2.5 μg of Lipofectin were added to 25 μl of serum-free DMEM separately and incubated at room temperature for 30 min. The DMEM containing the plasmid and Lipofectin was gently mixed and further incubated at room temperature for 15 min. Cells grown to 40% confluence in eight-well chamber slides were washed once with serum-free DMEM. The mixture was added to one well along with 150 μl of serum-free DMEM. Cells were incubated at 37°C for 5 h; then the medium was replaced with DMEM supplemented with 10% fetal bovine serum, 1% nonessential amino acids, 50 U of penicillin/ml, and 50 μg of streptomycin/ml.

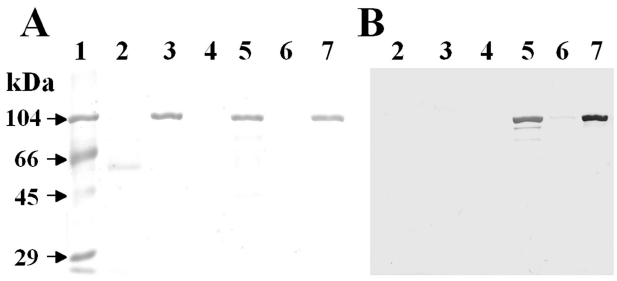

FIG. 1. Purification of EspC from a minimal clone and detection with a specific polyclonal antibody. (A) Detection of EspC and Pet (1 μg) from culture supernatants by SDS-PAGE. *espC* was previously cloned into pBAD30 and expressed in HB101. Supernatants of this construct were purified, as reported for Pet (shown in lane 3), from culture with glucose (lane 4) or arabinose (lane 5) through a 100-kDa-cutoff filter device. The EspC serine protease mutant (EspC S256I) was also obtained from culture with glucose (lane 6) or arabinose (lane 7). Concentrated supernatants from HB101 culture were used as a negative control (lane 2). Lane 1, molecular weight markers. (B) Detection of EspC by immunoblotting. Samples are placed as in panel A. EspC was detected by using a specific rabbit polyclonal antibody (dilution, 1:280).

Overlay assay. Two or four micrograms of protein (GST-fodrin, actin, tubulin, or bovine serum albumin [BSA]) or EspC was separated by sodium dodecyl sulfate–10% polyacrylamide gel electrophoresis (SDS–10% PAGE). These separated proteins were then transferred to nitrocellulose filters (Bio-Rad), which were blocked overnight in blocking buffer (150 mM NaCl, 8 mM Na_2HPO_4, 2 mM NaH_2PO_4 [pH 7.3], 2 mM $CaCl_2$, and 5% nonfat dry milk) at 4°C. Nitrocellulose membranes were then incubated for 1 h in buffer B (20 mM Tris-HCl, 150 mM NaCl, 0.1% Tween 20, 2 mM $CaCl_2$, and 5% bovine serum albumin) with either 5 μg of EspC/ml (for membranes containing GST-fodrin, actin, tubulin, or BSA) or 5 μg of GST-fodrin/ml (for membranes containing EspC) (1). All wash steps consisted of three 10-min incubations with blocking buffer. The strips were washed and then incubated for 1 h in blocking buffer with either a mouse polyclonal antiserum raised against GST (dilution, 1:1,000) or a rabbit polyclonal antiserum raised against EspC (dilution, 1:120). Following another wash step, the strips were incubated for 1 h in blocking buffer with an alkaline phosphatase (AP)-conjugated goat anti-rabbit antibody (dilution, 1:2,000) or an AP-conjugated goat anti-mouse antibody (dilution, 1:500) (both from Kirkegaard & Perry Laboratories, Gaithersburg, Md.). Following a final wash, binding was detected by using 1-Step NBT/BCIP (nitroblue tetrazolium–5-bromo-4-chloro-3-indolylphosphate) substrate (Pierce).

Degradation assay. Fifteen microliters (2.5 μg) of affinity-purified GST-fodrin was mixed with an equal volume of 2× digestion buffer (0.3 mM $CaCl_2$, 10 mM DTT) containing 1 μg of EspC, EspC S256I, or Pet. Reactions were carried out at 30°C at several time points and stopped by the addition of 4× SDS sample buffer. All samples were analyzed by SDS-PAGE. For inhibition experiments, EspC was preincubated with PMSF (2 mM) at 37°C for 30 min.

Western immunoblotting. Proteins from degradation assays were separated by SDS-PAGE, and protein bands were transferred to nitrocellulose membranes (27). Finally, the membranes were probed with anti-GST mouse polyclonal antibodies to detect GST-fodrin (1). The amino terminus of GST-fodrin was visualized with goat anti-mouse antibodies conjugated with AP (Kirkegaard & Perry Laboratories). Antigen-antibody reactions were developed by using the 1-Step NBT/BCIP substrate (Pierce).

RESULTS

Effects of EspC protein on HEp-2 epithelial cells. Mature EspC protein was partially purified from supernatants of the minimal clone HB101(pJLM174), grown in the presence of arabinose, through a 100-kDa cutoff filter device (Fig. 1A, lane 5). As a control we used the supernatant of HB101(pJLM174) grown in the presence of glucose, which represses *espC* expression (Fig. 1A, lane 4). HEp-2 cells were incubated for 4 h with EspC at various concentrations, starting with 40 μg/ml, the dose at which Pet causes cytotoxic effects. The appearance of the epithelial cells was not altered by treatment with concentrated supernatants from HB101(pJLM174) grown in the presence of glucose (which represses *espC* expression). In contrast to similarly purified Pet (Fig. 1A, lane 3), 40 μg of EspC/ml was not enough to produce a cytotoxic effect. After testing higher concentrations (80, 120, 180, and 240 μg/ml), we found that supernatants containing 180 μg of EspC/ml (~1 mM) caused damage to HEp-2 epithelial cells after 4 h of incubation. The damage observed under light microscopy was similar to that previously reported for Pet (21) and to that described below. To assess the time dependence of the EspC cytopathic effect on HEp-2 cells, cells were treated with 120 μg/ml (~900 nM) for 4, 6, 8, 10, or 12 h. The effects were time dependent (similar to those obtained when different doses were used), and the following morphological changes to epithelial cells were observed. After 4 h of interaction, the cells were practically unaffected (Fig. 2B) and were similar to untreated cells (Fig. 2A), whereas after 6 h, the cells were full of vacuoles within the cytoplasm (Fig. 2C). Moreover, after 8 h, the cell damage was characterized by cell contraction with apparent loss of cytoplasm (Fig. 2D). After 10 h of interaction with EspC, 50% of the cells were detached, and the remaining cells were rounded and showed membrane blebs (Fig. 2E). The last effects were similar to those observed for Pet at 40 μg/ml after 4 h of incubation (Fig. 2F). After 12 h of interaction with EspC, the cytoplasm could not be clearly defined, and nearly all HEp-2 cells were detached from the glass (data not shown). Thus, the effects of EspC observed under light microscopy were similar to those caused by Pet, but it was necessary to use three times the Pet concentration and 2.5 times the exposure time. In subsequent experiments, 120 μg of EspC/ml and 8 or 10 h of exposure were used to produce clear, highly reproducible effects, and for comparison, Pet was used at 40 μg/ml with 4 h of exposure.

Effects of EspC on the cytoskeleton. The cell-rounding phenotype suggests that EspC, as has been reported for Pet (21), disrupts the cytoskeleton or cytoskeleton-related proteins. To characterize the cytoskeletal effects, HEp-2 cells incubated with EspC were stained with rhodamine-labeled phalloidin and observed under confocal microscopy. Figure 3A shows rhodamine-labeled phalloidin staining of F-actin in untreated HEp-2 cells. These control cells were uniform and smooth-edged and showed organized linear-stress F-actin fibers. In contrast, HEp-2 cells treated with 120 μg of EspC/ml for 8 h revealed contraction of the cytoskeleton, loss of actin stress fibers, formation of surface blebs, and a globular appearance for some cells (Fig. 3B). Similar results were obtained when HEp-2 cells were treated with Pet (40 μg/ml) over 4 h (21) (Fig. 3E).

To test the role of serine protease activity in the toxic effects of EspC, the serine protease inhibitor PMSF, which has been shown to efficiently inhibit Pet serine protease activity (21), was used. When EspC was preincubated with 2 mM PMSF, the inhibitor abolished the cytoskeleton damage produced by EspC, as evidenced by the preservation of actin stress fibers (Fig. 3C), similar to those produced in untreated cells (Fig. 3A) and in cells treated with Pet that had been preincubated with PMSF (Fig. 3F). Additionally, a serine protease mutant of

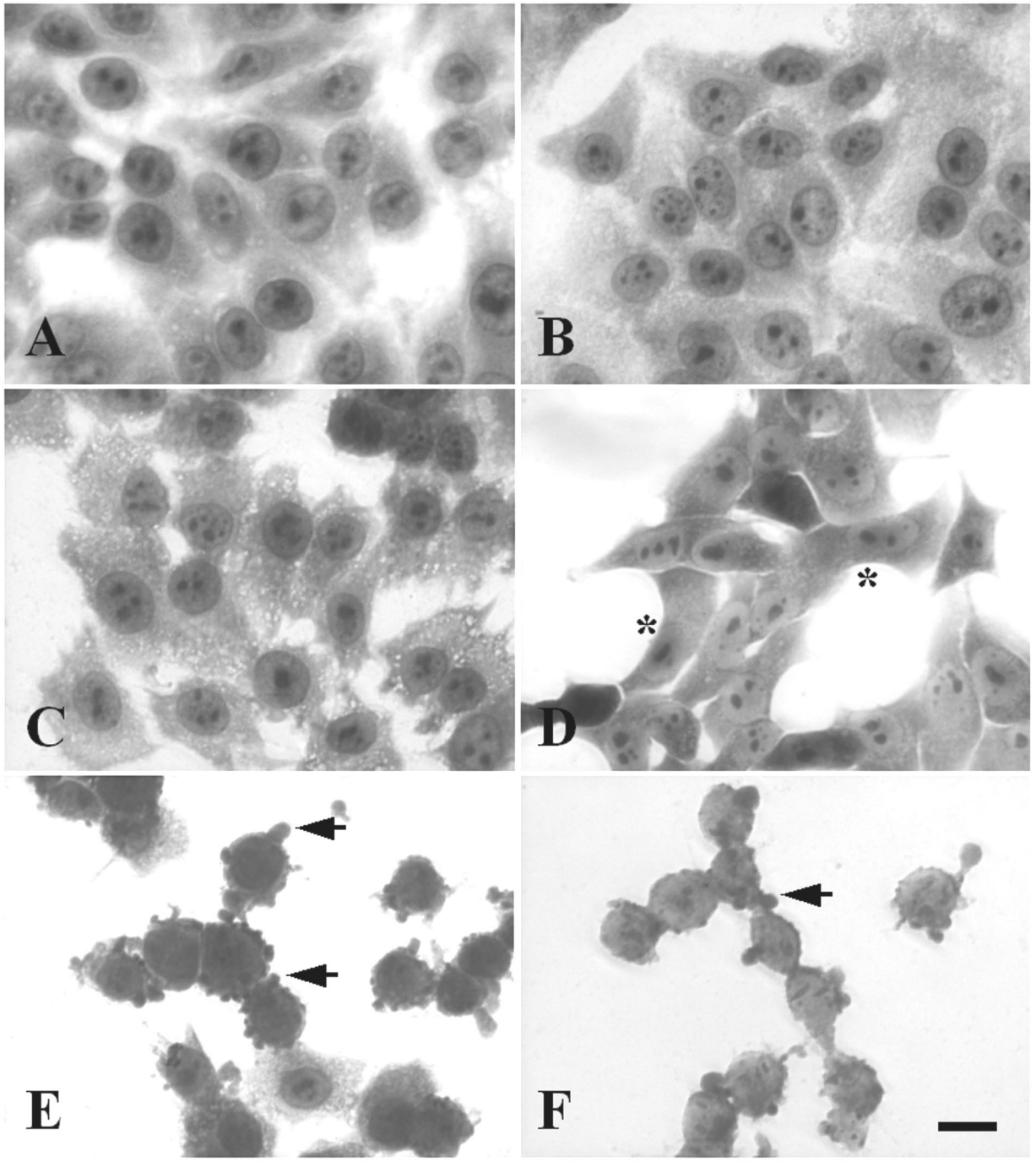

FIG. 2. EspC produces a cytotoxic effect on epithelial cells. HEp-2 cells were treated with EspC (120 μg/ml) for different times or with Pet (40 μg/ml) for 4 h. Then the cells were fixed and stained with Giemsa stain. Slides were observed under a light microscope. Cells were either left untreated (A) or treated with EspC for 4 h (B), 6 h (C), 8 h (D), or 10 h (E). The cytotoxic effect caused by Pet (F) was used as a positive control. Asterisks indicate the beginning of cell contraction; arrows point to membrane blebs.

EspC was constructed by changing the serine at position 256 to an isoleucine residue (EspC S256I) and was expressed in HB101 (Fig. 1A, lane 7). This mutant, like the Pet S260I mutant (21), was unable to cause cytoskeletal damage (Fig. 3D). Moreover, no effect was seen when HEp-2 cells were preincubated with PMSF before addition of the toxin (data not shown), suggesting that the serine protease activity is directly conferred by the EspC protein and not by proteins from the epithelial cells.

Internalization of EspC protein into epithelial cells. Recently, it has been shown that Pet must enter the epithelial cell in order to produce its cytotoxic effects (19). In order to explore this possibility for EspC, we performed cellular fractionation of HEp-2 cells treated with EspC, as well as immuno-

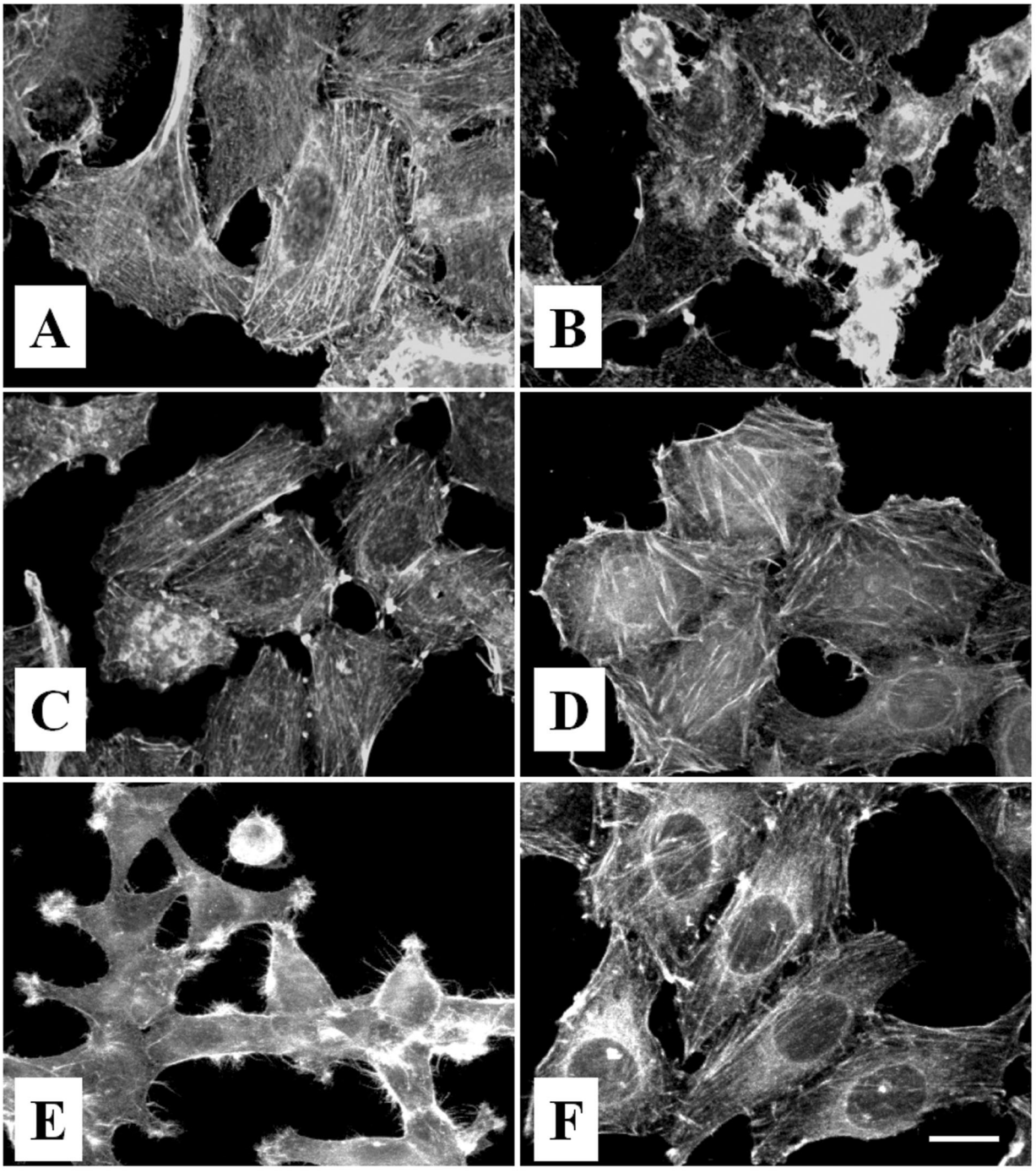

FIG. 3. EspC causes cytoskeletal damage through its serine protease motif. HEp-2 cells were treated with EspC (120 μg/ml) for 8 h. For inhibition experiments, EspC was preincubated with 2 mM PMSF for 15 min and then added to HEp-2 cells, or cells were treated with the serine protease mutant (EspC S260I). (A) Untreated cells in the presence of 2 mM PMSF; (B) cells treated with EspC; (C) cells treated with EspC preincubated with 2 mM PMSF; (D) cells treated with EspC S256I; (E) cells treated for 4 h with Pet (40 μg/ml); (F) cells treated for 4 hr with Pet preincubated with 2 mM PMSF.

blotting with anti-EspC polyclonal antibodies (Fig. 1B, lane 5), which have no cross-reactivity with Pet (Fig. 1B, lane 3). EspC protein was found in lysates of HEp-2 cells showing cytotoxic effects, and cellular fractionation showed that EspC was located in both the cytoplasmic and membrane fractions (data not shown). It is noteworthy that Pet toxin has been located mainly in the cytoplasmic fraction, with a sparse Pet-reactive band seen in the membrane fraction (19).

To further visualize EspC internalization, HEp-2 cells treated with EspC for 4 to 10 h were fixed, permeabilized, incubated first with anti-EspC polyclonal antibodies and then with fluorescein-labeled goat anti-rabbit IgG, and observed

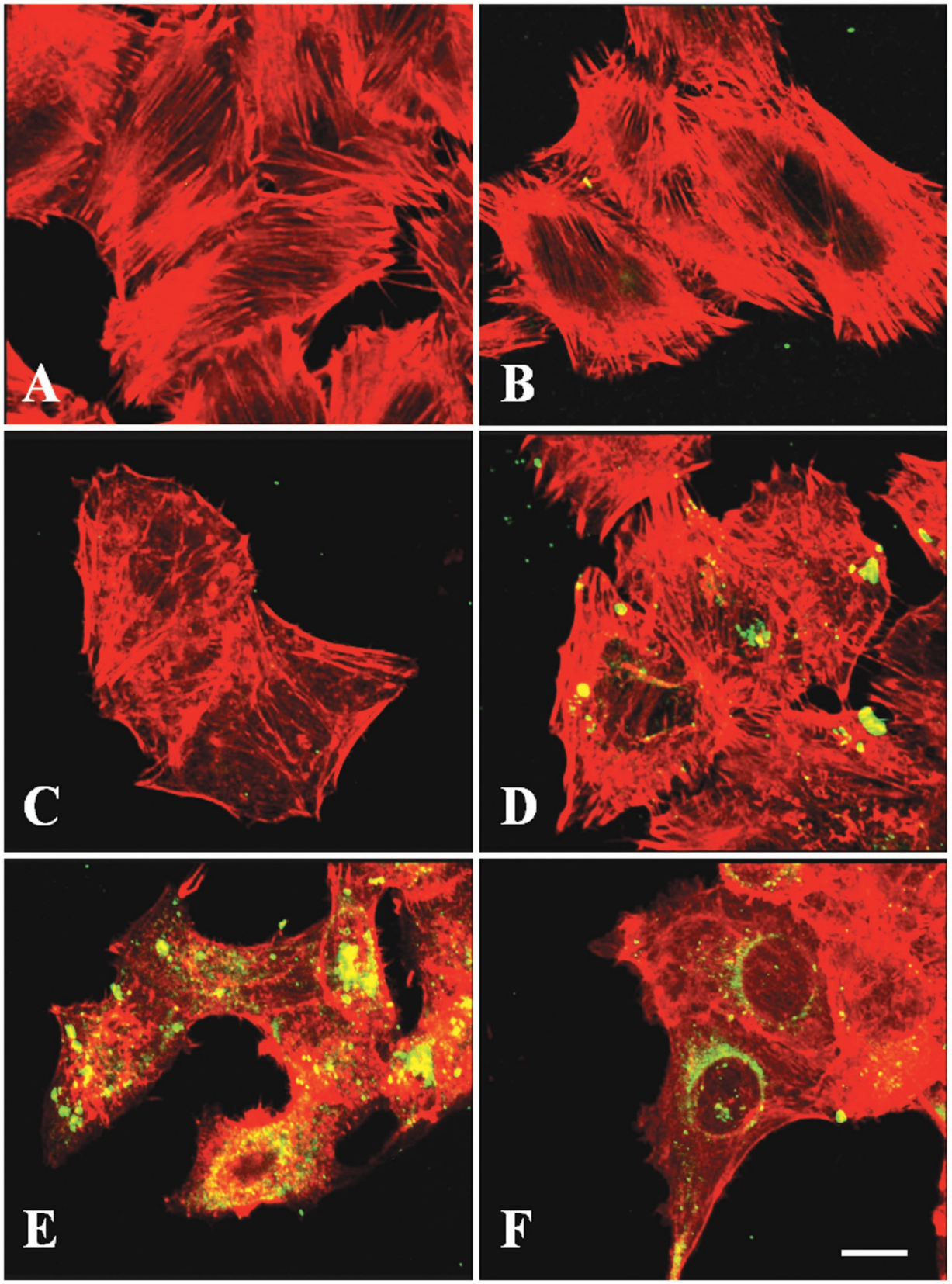

FIG. 4. Internalization of EspC within epithelial cells. HEp-2 cells were treated with EspC (120 μg/ml) for different times or with Pet (40 μg/ml) for 1 h. Cells were fixed and stained with rhodamine-phalloidin and anti-EspC (or anti-Pet) antibodies and a secondary fluorescein-labeled anti-rabbit antibody. Slides were observed by confocal microscopy. Cells were either left untreated (A) or treated with EspC for 2 h (B), 4 h (C), 6 h (D), or 8 h (E). Pet was used as a positive control (F).

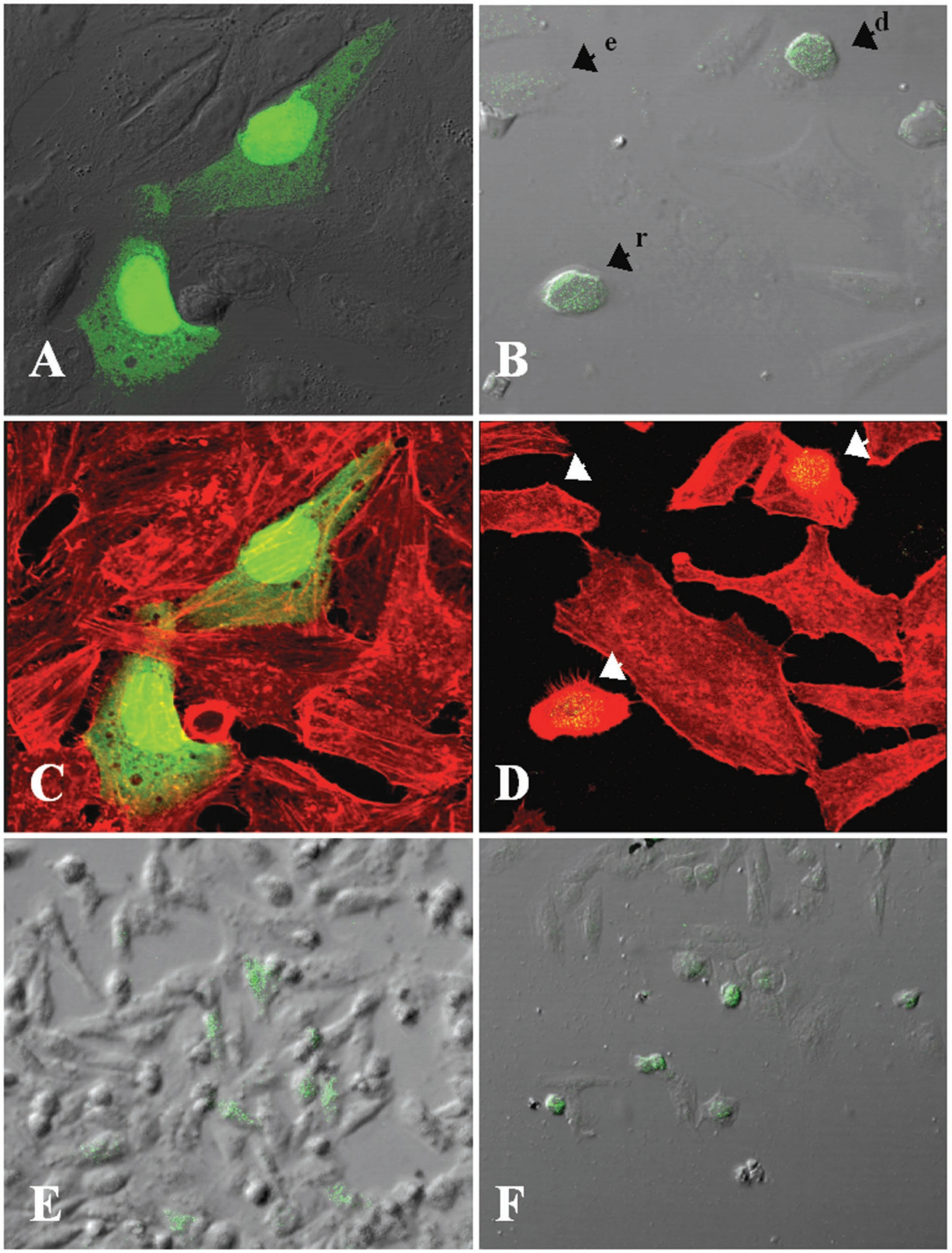

FIG. 5. Cytoskeletal damage in epithelial cells transfected with GFP-*espC*. GFP-*espC*-transfected cells were fixed 36 h posttransfection and stained with rhodamine-phalloidin. Slides were observed by confocal microscopy. (A and B) GFP-expressing control cells (A) and GFP-EspC-expressing cells (B) were visualized by confocal microscopy and merged with cell images obtained by Nomarski microscopy. Arrowheads point to damaged cells: e, elongated cell; d, detached cell; r, rounding cell. (C and D) GFP-expressing control cells (C) and GFP-EspC-expressing cells (D) were also visualized by confocal microscopy and merged with the red channel showing the actin cytoskeleton stained with rhodamine-phallodin. (E and F) The cytotoxic effect of EspC is obvious when GFP-expressing control cells (E) and GFP-EspC-expressing cells (F) are observed at a low magnification.

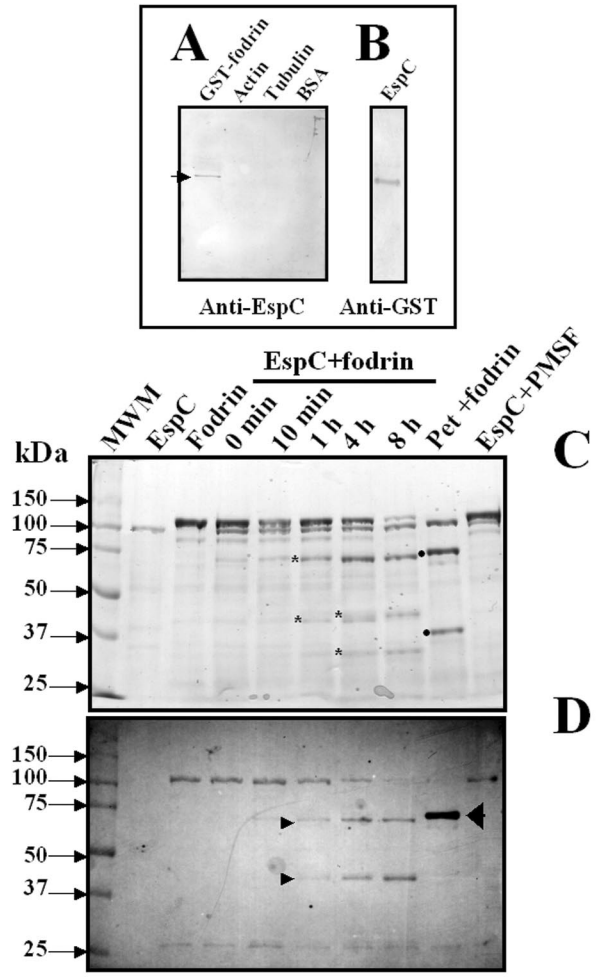

FIG. 6. EspC binds to and degrades human fodrin in vitro. (A and B) Interaction of fodrin and EspC as determined by an overlay assay. GST-fodrin, actin, tubulin, and BSA (A) and EspC (B) were separated by SDS-PAGE and transferred to nitrocellulose membranes. The membrane containing the proteins in panel A was incubated with EspC (5 μg/ml), and the membrane containing EspC was incubated with GST-fodrin (5 μg/ml), for 1 h. The affinity reaction was revealed by using anti-EspC or anti-GST antibodies and AP-labeled anti-rabbit or anti-mouse antibodies. (C and D) Degradation assay. Purified GST-fodrin (2.5 μg) was incubated with EspC (1 μg) for different times or with Pet (1 μg) for 1 h and then separated by SDS-PAGE (C). Samples were placed as indicated above each lane. Asterisks indicate subproducts of fodrin degradation by EspC (72, 45, 43, and 34 kDa); solid dots indicate those produced by Pet (74 and 37 kDa). MWM, molecular weight marker. Samples similar to those in panel A were analyzed by Western blotting (D). Nitrocellulose membranes were revealed with anti-GST antibodies by using AP-labeled anti-mouse antibodies.

under confocal microscopy. These experiments showed that during the first 6 h of incubation with EspC, the anti-EspC antibodies react with intracellular structures and structures on the cell membrane (Fig. 4D), corresponding to the presence of EspC in the membrane and cytoplasmic fractions. Pet has been observed inside epithelial cells after 15 to 30 min of exposure (19) and around the nuclei after 1 h of incubation (Fig. 4F). Further, after 8 h of incubation, EspC was found inside epithelial cells, and the cytoskeletal damage became evident (Fig. 4E). In contrast, the cytoskeletal damage caused by Pet began around 2 h after exposure (21).

Cytoskeletal effect produced in EspC-expressing HEp-2 cells. To further explore if the internalization process is required in order to produce cytoskeletal damage, HEp-2 cells were transfected with the *espC* gene inserted into pcDNA3.1/CT-GFP-TOPO. The cytoskeletons of the transfected cells were stained with TRITC-phalloidin. Vector-transfected cells were normal in appearance, expressing green fluorescent protein (GFP) inside (Fig. 5A and C). GFP-*espC*-transfected HEp-2 cells showed cytotoxic effects: expression of GFP-EspC fluorescence occurred in elongated, rounding, or detached cells (Fig. 5B), which exhibited cytoskeletal damage (Fig. 5D). Neighboring cells which were not transfected with GFP-*espC* revealed neither green florescence nor cytoskeletal damage (Fig. 5B and D). Interestingly, when a lower magnification was used, only the GFP-*espC*-transfected cells were rounded (Fig. 5F), while all vector-transfected cells containing green fluorescence were normal (Fig. 5E). All these data suggest that EspC internalization is needed to produce the cytoskeletal damage leading to cell detachment from the substratum.

Interaction of EspC with fodrin. Since Pet has affinity with α-fodrin (formally named αII spectrin) and disrupts fodrin organization, leading to cytoskeletal effects (1), we decided to investigate whether EspC is able to produce the same effects. To address this question, we performed binding experiments with EspC and either fodrin, actin, tubulin, or BSA by overlay analyses. When recombinant α-fodrin containing repeats 8 to 14 fused to GST (109 kDa) was immobilized in nitrocellulose membranes, EspC was able to bind to this 109-kDa protein (as revealed by anti-EspC antibodies) but not to actin, tubulin, or BSA (Fig. 6A), suggesting a specific affinity of EspC for fodrin. Moreover, when EspC was immobilized in the membrane, fodrin was also able to bind to the 110-kDa protein (EspC), as revealed by anti-GST antibodies (Fig. 6B).

Recently, it has been shown that Pet degrades fodrin, causing fodrin redistribution in HEp-2 cells, and that the cleavage site on fodrin is highly specific for the Pet serine protease motif (1). Since EspC has affinity for fodrin, we investigated whether EspC is able to produce fodrin redistribution. To address this issue, HEp-2 cells were incubated with EspC for different times, and the actin cytoskeleton and fodrin were stained in order to observe their redistribution. Staining of control cells with anti-fodrin antibodies revealed small fluorescent spots along the epithelial cell, whereas staining with rhodamine-phalloidin showed the classical array of actin-containing stress fibers (Fig. 7A). When cells were treated with EspC for 2, 4, 6, 8, or 10 h, fodrin distribution was not affected (Fig. 7B to F), even when the actin cytoskeleton was visibly damaged after 8 and 10 h of exposure (Fig. 7E and F). In contrast, a clear change in both fodrin and actin distribution was observed after 2 h of exposure to Pet. Fodrin was redistributed to form intracellular aggregates, which were located in membrane blebs, and the actin cytoskeleton was also aggregated into different blebs (Fig. 7G), as previously reported (1). Interestingly, trypsin, which is unable to enter the cell, had no effect on fodrin distribution (Fig. 7H). The integrity of the actin cytoskeleton and the cell-rounding effects were similar to those seen with EspC. These data suggest that EspC did not produce redistribution of fodrin in epithelial cells, as Pet did.

To further explore whether EspC is able to cleave fodrin, we performed in vitro degradation experiments using recombinant

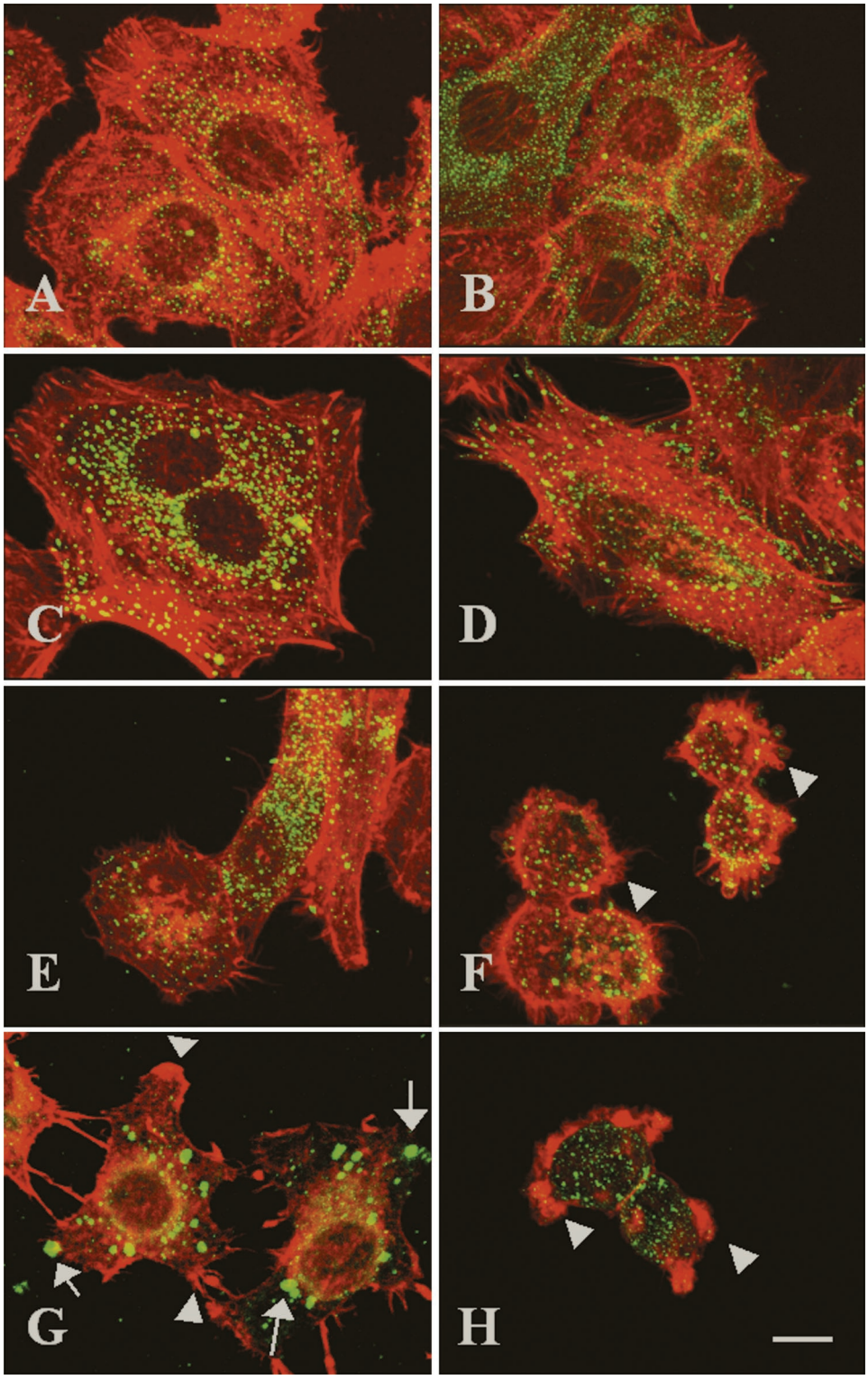

FIG. 7. Effects of EspC on fodrin redistribution in epithelial cells. HEp-2 cells were treated either with EspC (120 μg/ml) for 2, 4, 6, 8,or 10 h (B through F, respectively), with Pet (40 μg/ml) for 4 h (G), or with trypsin (0.4 μg/ml) for 1 h (H); untreated cells were used as a control (A). Cells were then fixed and subsequently stained simultaneously with rhodamine-phalloidin, anti-α-fodrin antibodies, and a fluorescein-labeled secondary anti-goat antibody. Slides were observed by confocal microscopy. Arrows indicate fodrin accumulation (green fluorescence). Arrowheads point to actin aggregates (red fluorescence).

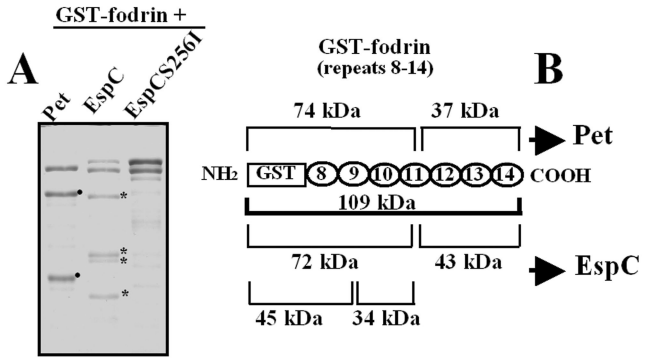

FIG. 8. An EspC serine protease motif mutant is unable to cleave fodrin. (A) Cleavage of GST-fodrin by EspC or EspC S256I. Purified GST-fodrin (2.5 μg) was incubated with Pet, EspC, or EspC S256I (1 μg) for 4 h and then separated by SDS-PAGE. Asterisks indicate subproducts of GST-fodrin degradation by EspC (72, 45, 43 and 34 kDa); solid dots indicate those produced by Pet (74 and 37 kDa). (B) Subproducts of GST-fodrin generated by Pet and EspC. Schematic representation of GST-fodrin shows the subproducts produced by Pet and EspC considering the amino acid sequences of the repetitive units of fodrin and GST.

GST-fodrin, which has been shown to be a substrate of the Pet serine protease motif (1). GST-fodrin (109 kDa) was exposed to EspC for several times and then resolved by SDS-PAGE. At time zero, fodrin and EspC were detected as two main bands with apparent molecular sizes of 115 and 110 kDa, respectively (Fig. 6C). After 10 min, the intensity of the 109-kDa band corresponding to GST-fodrin started to decrease, and after 8 h, it almost disappeared (Fig. 6C). At the same times, new bands of minor molecular weights appeared; after 1 h, two new bands with apparent molecular sizes of 72 and 43 kDa were observed, whereas after 4 h, two new bands of 45 and 34 kDa were observed (Fig. 6C). The new bands appeared to be breakdown products of GST-fodrin, because the band corresponding to EspC was maintained during the experiment (from 0 min to 8 h). Moreover, preincubation of EspC with PMSF prevented fodrin degradation, and the breakdown products were not seen (Fig. 6C, last lane). Interestingly, the subproducts of fodrin generated by EspC were different from those generated by Pet, which had molecular sizes of 74 and 36 kDa upon SDS-PAGE (Fig. 6C). These data strongly suggest that by using their serine protease motifs, EspC caused two cleavages in fodrin while Pet caused only one cleavage in the same substrate. To confirm the role of the serine protease motif in the cleavage of fodrin, GST-fodrin was incubated with the EspC S256I mutant, which was unable to cleave it (Fig. 8A). In contrast, EspC-treated GST-fodrin showed four bands generated by its cleavage at two sites (Fig. 8A).

To determine the proteolytic cleavage site in GST-fodrin, we used antibodies against GST to identify which of the subproducts were recognized by these antibodies, since GST protein is fused to the amino-terminal region of the recombinant fodrin. The degradation assay was analyzed by Western blotting. After 1 h of incubation, the anti-GST antibody recognized the 72-kDa subproduct, and after 4 h of incubation, it recognized the 45-kDa subproduct (Fig. 6D). These data indicate that the 72-kDa fragment was further cleaved to produce the fragment of 45 kDa, again suggesting two cleavage sites on fodrin for EspC. In contrast, in Pet-treated GST-fodrin, the antibodies against GST recognized only the 74-kDa band and no further bands, indicating one cleavage site on fodrin for Pet (Fig. 6D). Since each structural repeat unit of fodrin is about 11.6 kDa, these data also suggest that the EspC cleavage sites may occur within the 11.6 kDa of fodrin's 11th structural repeat unit to produce the 72-kDa fragment and within the 9th structural repeat to produce the 45-kDa fragment (Fig. 8B).

Competition experiments to cause cytoskeletal damage. To compare the mechanisms of action of EspC and Pet, we tested whether an excess of Pet S260I blocks the cytoskeletal damage caused by EspC and whether an excess of EspC S256I blocks the cytoskeletal damage caused by Pet. As had been previously demonstrated for Pet S260I (1, 19), EspC S256I also was able to enter epithelial cells but unable to produce cytoskeletal damage (Fig. 9C), as opposed to native EspC, which caused clear cytoskeletal damage in epithelial cells (Fig. 9B). An excess of EspC S256I added 30 min before Pet addition prevented neither Pet entry into cells nor cytoskeletal damage (Fig. 9E). Similarly, an excess of Pet S260I was unable to prevent either EspC entry into cells or cytoskeletal damage (Fig. 9F). However, an excess of EspC S256I added 30 min before native EspC addition did prevent cytoskeletal damage (Fig. 9G); similarly, when both the EspC and Pet serine protease motif mutants were used, they were unable to cause cytoskeletal damage (Fig. 9H). Thus, only EspC S256I competes with native EspC to prevent cytoskeletal damage, indicating that EspC acts on epithelial cells through a mechanism different from that of Pet toxin.

DISCUSSION

EPEC strains are an extremely common cause of diarrhea in young children throughout the developing world. However, the mechanism by which diarrhea caused by EPEC occurs is unclear. Even when a possible explanation might be the decreased absorption due to pedestal formation, the roles of microvillus effacement and pedestal formation in the disease remain undefined (3). Secretion of chloride, a common effect of bacterial enterotoxins, has been shown in EPEC infection, but no enterotoxin had been implicated (2). Recently, EspC, an autotransporter protein which does not participate in signal transduction and pedestal formation (25), has been shown to have enterotoxic activity (17). EspC is a member of the SPATE

FIG. 9. EspC S256I, but not Pet S260I, competes with EspC by blocking cytoskeletal damage. HEp-2 cells were treated with 120 μg of EspC or EspC S256I/ml (B and C, respectively) or with 37 μg of Pet/ml (D). In competition experiments, HEp-2 cells were first treated with an excess (220 μg/ml) of EspC S256I for 30 min and then with 37 μg of Pet/ml for 3 h (E) or 120 μg of EspC/ml for 9 h (G). HEp-2 cells were also first treated with an excess (70 μg/ml) of Pet S260I for 30 min and then with 120 μg of EspC or EspC S256I/ml (F and H, respectively) for 9 h. Untreated cells was used as a control (A). After treatment, the cells were fixed, stained simultaneously with rhodamine-phalloidin and anti-EspC or anti-Pet antibodies, and then stained with fluorescein-labeled anti-rabbit antibodies. Slides were observed by confocal microscopy.

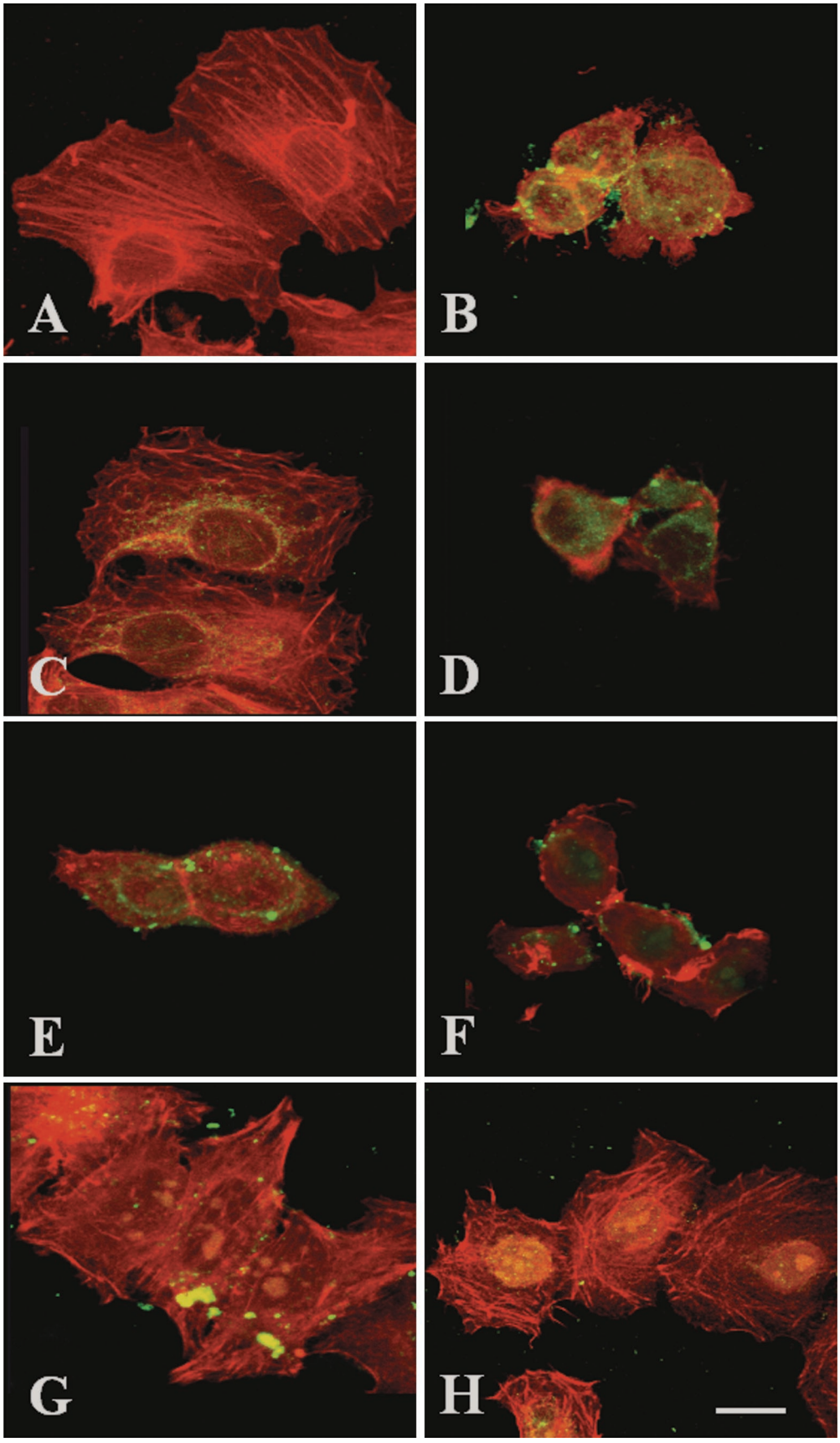
A
B
C
D
E
F
G
H

subfamily carrying the same serine protease motif sequence as the Pet toxin. This serine protease motif confers enterotoxic and cytotoxic activities on Pet (21). Here we show that EspC also produces cytotoxic effects on epithelial cells, and under light microscopy the cell damage appears to be similar to that previously reported for Pet (21). However, the cell damage was reached only at a dose of EspC three times (120 μg/ml) higher than that used for Pet (40 μg/ml) and at three-times-longer incubation times. As with Pet, the cell damage was characterized by cell contraction and cell detachment and was also due to disruption of the actin cytoskeleton. These effects were caused by the serine protease motif, as evidenced by the fact that the serine protease inhibitor PMSF and an EspC serine protease motif mutant (EspC S256I) abolished the cytoskeletal damage, which was characterized by perinuclear contraction of F-actin and loss of stress fibers, similar to that caused by Pet (21).

Since the effects on the cytoskeleton caused by Pet depend on its internalization (19), we explored this possibility for EspC. Interestingly, cellular fractionation of EspC-treated epithelial cells showed that EspC was found in the membrane and cytoplasmic fractions (data not shown), while Pet was found mainly in the cytoplasmic fraction (19). By confocal microscopy, EspC was found inside epithelial cells, but this process occurred after ca. 6 h (versus 30 min for Pet), suggesting that the intracellular trafficking may be different from that for Pet. However, the internalization process is required for production of cytoskeletal damage, because when EspC was not inside the cells, the cytoskeleton was preserved. Indeed, when eukaryotic epithelial cells were transfected by using the functional domain of EspC fused to GFP, all the GFP-EspC-expressing cells showed cytoskeletal damage as visualized by confocal microscopy, whereas epithelial cells transfected with GFP alone (vector) did not, even when GFP was expressed inside the cells. On the other hand, it is noteworthy that the confocal micrographs showed that EspC was found inside the cell as well as on the cell membrane, as we had previously seen by cellular fractionation, suggesting that in contrast to Pet, EspC was not efficiently internalized. On the other hand, after EspC internalization (which occurred around 6 h), cytoskeletal damage was observed around 8 to 9 h, while Pet was seen inside the cells between 15 and 30 min and cytoskeletal damage occurred around 3 h (19). This suggests that for both proteins, once they are inside the cell, intracellular trafficking and damage to their target occur in about 3 h. Experiments are in progress to address the question of whether receptor affinity and intracellular trafficking are different in Pet versus EspC.

Another effect produced by the Pet serine protease motif occurs in the intracellular protein target, fodrin, which is cleaved on its calmodulin-binding domain (1), leading to fodrin redistribution, which explains the cytoskeletal damage. Although fodrin is degraded by EspC, this effect is not accompanied by fodrin redistribution. Thus, the lack of fodrin redistribution could be due to the fact that EspC has different cleavage sites on fodrin than Pet. Pet cleaves recombinant fodrin within the calmodulin-binding domain between M1198 and V1199, producing two fragments observed in SDS-PAGE as two subproduct bands of 74 and 37 kDa (1). While EspC generates four subproducts with apparent molecular weights of 72, 43, 45, and 34 kDa, the last two fragments come from further processing of an initial fragment of 72 kDa (Fig. 6). Moreover, like that by Pet, these cleavages of fodrin by EspC also depend on the serine protease motif; no cleavage of recombinant fodrin occurred when mutant forms of Pet and EspC with mutations of this motif were used, and the effect was also blocked by PMSF preincubation.

On the other hand, the fact that Pet, but not EspC, cleaves within the fodrin calmodulin-binding domain perhaps is related to the mechanism of action of Pet on the protein target, since calmodulin and calpain I coordinately regulate the interaction of fodrin with actin to maintain cytoskeletal integrity (6). In contrast, the EspC cleavage sites occur outside of the calmodulin-binding domain, even though one cleavage site is close to this domain. The importance of the cleavage site on fodrin (αII spectrin) is due to the fact that the proteolysis of fodrin by calcium-dependent proteases has been observed during several processes, and this proteolysis leads to various necrotic and apoptotic events (28). Thus, αII spectrin is alternatively cleaved by calpain and caspase 3. Both proteases cleave at adjacent sites in repeat 11, near the calmodulin-binding domain, to produce two nonidentical breakdown subproducts of 150 kDa (with different N termini): calpain cleaves between V_{1176} and G_{1177}, and the caspase 3 cleavage site is between D_{1185} and S_{1186}. Calpain subsequently cleaves this region again, between G_{1230} and S_{1231}, producing a slightly smaller breakdown subproduct of 145 kDa. In addition, caspase 3 cleaves in repeat 13, between D_{1478} and S_{1479}, producing the apoptosis-specific breakdown subproduct of 120 kDa (28). Analogously, differential Pet and EspC cleavages on αII spectrin could mean different biological events.

Additionally, taking advantage of the fact that Pet S260I and EspC S256I are able to enter epithelial cells but unable to damage the actin cytoskeleton, cleave fodrin, or produce cytotoxic effects, we used them to perform competition experiments with the native proteins by measuring cytoskeletal damage. Clearly, an excess of EspC S256I was able to block the cytoskeletal damage caused by EspC but unable to block the cytoskeletal damage caused by Pet. Moreover, Pet S260I was also unable to prevent the cytoskeletal damage caused by EspC. These data indicate that EspC and Pet have different ways of causing cytoskeletal damage.

It is clear that EspC and Pet have different activities on epithelial cells. Further analyses are in progress in an effort to understand the role of EspC in EPEC pathogenesis, its interaction with fodrin, and its intracellular trafficking. Even though both these proteins of the SPATE subfamily have the same serine protease motif, this work clearly shows that EspC is deficient in gaining entry into HEp-2 cells compared to Pet, and it suggests that the conformational structure of the protein is important for the activity of the catalytic site, since it can influence the interaction with the target protein. Thus, differences in internalization, trafficking, and activity on the target protein between the two proteins may explain the reduced ability of EspC to cause cytotoxic effects. However, this mechanism of EspC may play a specialized role in the pathogenesis of EPEC, which may be different from the role of Pet in the pathogenesis of EAEC.

ACKNOWLEDGMENTS

This work was supported by a grant from the Consejo Nacional de Ciencia y Tecnología de México (CONACYT, 30004 M) to F.N.-G.

We thank Rocio Huerta and José Luna for technical help.

REFERENCES

1. **Canizalez-Roman, A., and F. Navarro-Garcia.** 2003. Fodrin CaM-binding domain cleavage by Pet from enteroaggregative *Escherichia coli* leads to actin cytoskeletal disruption. Mol. Microbiol. **48:**947–958.
2. **Collington, G. K., I. W. Booth, and S. Knutton.** 1998. Rapid modulation of electrolyte transport in Caco-2 cell monolayers by enteropathogenic *Escherichia coli* (EPEC) infection. Gut **42:**200–207.
3. **Donnenberg, M. S., J. B. Kaper, and B. B. Finlay.** 1997. Interactions between enteropathogenic *Escherichia coli* and host epithelial cells. Trends Microbiol. **5:**109–114.
4. **Elliott, S. J., L. A. Wainwright, T. K. McDaniel, K. G. Jarvis, Y. K. Deng, L. C. Lai, B. P. McNamara, M. S. Donnenberg, and J. B. Kaper.** 1998. The complete sequence of the locus of enterocyte effacement (LEE) from enteropathogenic *Escherichia coli* E2348/69. Mol. Microbiol. **28:**1–4.
5. **Eslava, C., F. Navarro-Garcia, J. R. Czeczulin, I. R. Henderson, A. Cravioto, and J. P. Nataro.** 1998. Pet, an autotransporter enterotoxin from enteroaggregative *Escherichia coli*. Infect. Immun. **66:**3155–3163.
6. **Harris, A. S., and J. S. Morrow.** 1990. Calmodulin and calcium-dependent protease I coordinately regulate the interaction of fodrin with actin. Proc. Natl. Acad. Sci. USA **87:**3009–3013.
7. **Jarvis, K. G., J. A. Giron, A. E. Jerse, T. K. McDaniel, M. S. Donnenberg, and J. B. Kaper.** 1995. Enteropathogenic *Escherichia coli* contains a putative type III secretion system necessary for the export of proteins involved in attaching and effacing lesion formation. Proc. Natl. Acad. Sci. USA **92:**7996–8000.
8. **Jerse, A. E., and J. B. Kaper.** 1991. The *eae* gene of enteropathogenic *Escherichia coli* encodes a 94-kilodalton membrane protein, the expression of which is influenced by the EAF plasmid. Infect. Immun. **59:**4302–4309.
9. **Jerse, A. E., J. Yu, B. D. Tall, and J. B. Kaper.** 1990. A genetic locus of enteropathogenic *Escherichia coli* necessary for the production of attaching and effacing lesions on tissue culture cells. Proc. Natl. Acad. Sci. USA **87:**7839–7843.
10. **Kenny, B., R. DeVinney, M. Stein, D. J. Reinscheid, E. A. Frey, and B. B. Finlay.** 1997. Enteropathogenic *E. coli* (EPEC) transfers its receptor for intimate adherence into mammalian cells. Cell **91:**511–520.
11. **Kenny, B., L. C. Lai, B. B. Finlay, and M. S. Donnenberg.** 1996. EspA, a protein secreted by enteropathogenic *Escherichia coli*, is required to induce signals in epithelial cells. Mol. Microbiol. **20:**313–323.
12. **Knutton, S., I. Rosenshine, M. J. Pallen, I. Nisan, B. C. Neves, C. Bain, C. Wolff, G. Dougan, and G. Frankel.** 1998. A novel EspA-associated surface organelle of enteropathogenic *Escherichia coli* involved in protein translocation into epithelial cells. EMBO J. **17:**2166–2176.
13. **Knutton, S., R. K. Shaw, M. K. Bhan, H. R. Smith, M. M. McConnell, T. Cheasty, P. H. Williams, and T. J. Baldwin.** 1992. Ability of enteroaggregative *Escherichia coli* strains to adhere in vitro to human intestinal mucosa. Infect. Immun. **60:**2083–2091.
14. **Lai, L. C., L. A. Wainwright, K. D. Stone, and M. S. Donnenberg.** 1997. A third secreted protein that is encoded by the enteropathogenic *Escherichia coli* pathogenicity island is required for transduction of signals and for attaching and effacing activities in host cells. Infect. Immun. **65:**2211–2217.
15. **McDaniel, T. K., and J. B. Kaper.** 1997. A cloned pathogenicity island from enteropathogenic *Escherichia coli* confers the attaching and effacing phenotype on *E. coli* K-12. Mol. Microbiol. **23:**399–407.
16. **McNamara, B. P., and M. S. Donnenberg.** 1998. A novel proline-rich protein, EspF, is secreted from enteropathogenic *Escherichia coli* via the type III export pathway. FEMS Microbiol. Lett. **166:**71–78.
17. **Mellies, J. L., F. Navarro-Garcia, I. Okeke, J. Frederickson, J. P. Nataro, and J. B. Kaper.** 2001. *espC* pathogenicity island of enteropathogenic *Escherichia coli* encodes an enterotoxin. Infect. Immun. **69:**315–324.
18. **Moon, H. W., S. C. Whipp, R. A. Argenzio, M. M. Levine, and R. A. Giannella.** 1983. Attaching and effacing activities of rabbit and human enteropathogenic *Escherichia coli* in pig and rabbit intestines. Infect. Immun. **41:**1340–1351.
19. **Navarro-Garcia, F., A. Canizalez-Roman, J. Luna, C. Sears, and J. P. Nataro.** 2001. Plasmid-encoded toxin of enteroaggregative *Escherichia coli* is internalized by epithelial cells. Infect. Immun. **69:**1053–1060.
20. **Navarro-Garcia, F., C. Eslava, J. M. Villaseca, R. Lopez-Revilla, J. R. Czeczulin, S. Srinivas, J. P. Nataro, and A. Cravioto.** 1998. In vitro effects of a high-molecular-weight heat-labile enterotoxin from enteroaggregative *Escherichia coli*. Infect. Immun. **66:**3149–3154.
21. **Navarro-Garcia, F., C. Sears, C. Eslava, A. Cravioto, and J. P. Nataro.** 1999. Cytoskeletal effects induced by Pet, the serine protease enterotoxin of enteroaggregative *Escherichia coli*. Infect. Immun. **67:**2184–2192.
22. **Neves, B. C., S. Knutton, L. R. Trabulsi, V. Sperandio, J. B. Kaper, G. Dougan, and G. Frankel.** 1998. Molecular and ultrastructural characterisation of EspA from different enteropathogenic *Escherichia coli* serotypes. FEMS Microbiol. Lett. **169:**73–80.
23. **Pohlner, J., R. Halter, K. Beyreuther, and T. F. Meyer.** 1987. Gene structure and extracellular secretion of *Neisseria gonorrhoeae* IgA protease. Nature **325:**458–462.
24. **Stabach, P. R., C. D. Cianci, S. B. Glantz, Z. Zhang, and J. S. Morrow.** 1997. Site-directed mutagenesis of alpha II spectrin at codon 1175 modulates its mu-calpain susceptibility. Biochemistry **36:**57–65.
25. **Stein, M., B. Kenny, M. A. Stein, and B. B. Finlay.** 1996. Characterization of EspC, a 110-kilodalton protein secreted by enteropathogenic *Escherichia coli* which is homologous to members of the immunoglobulin A protease-like family of secreted proteins. J. Bacteriol. **178:**6546–6554.
26. **Taylor, K. A., C. B. O'Connell, P. W. Luther, and M. S. Donnenberg.** 1998. The EspB protein of enteropathogenic *Escherichia coli* is targeted to the cytoplasm of infected HeLa cells. Infect. Immun. **66:**5501–5507.
27. **Towbin, H., T. Staehelin, and J. Gordon.** 1979. Electrophoretic transfer of proteins from polyacrylamide gels to nitrocellulose sheets: procedure and some applications. Proc. Natl. Acad. Sci. USA **76:**4350–4354.
28. **Wang, K. K.** 2000. Calpain and caspase: can you tell the difference? Trends Neurosci. **23:**20–26.

Editor: J. T. Barbieri